

A demonstration of the capabilities of multisatellite observations of oceanic lightning

W. L. Boeck,¹ D. M. Suszcynsky,² T. E. Light,² A. R. Jacobson,² H. J. Christian,³ S. J. Goodman,³ D. E. Buechler,⁴ and J. L. L. Guillen⁵

Received 30 December 2003; revised 12 April 2004; accepted 18 June 2004; published 8 September 2004.

[1] We have examined lightning flashes in five nighttime, oceanic thunderstorms, which were jointly observed by Tropical Rainfall Measuring Mission (TRMM) and Fast On-Orbit Recording of Transient Events (FORTE). The multiplicity of instruments on board these satellites presents a multiphenomenological snapshot view of oceanic nighttime convection. Data are available for five oceanic storms with a total of 40 flashes. The independent optical imagers on each satellite establish the flash locations. The relative fraction of Lightning Imaging Sensor (LIS)–detected optical pulses that were also observed by the FORTE/photodiode detector varied from 0% for LIS range less than $10^4 \text{ J sr}^{-1} \text{ m}^{-2} \mu\text{m}^{-1}$ to 100% for LIS range greater than $10^6 \mu\text{J}^{-1} \text{ sr}^{-1} \text{ m}^{-2} \mu\text{m}^{-1}$. The FORTE/VHF data sometimes allow estimation of the VHF source emissions heights and identification of individual discharge processes as positive or negative, in-cloud or cloud-to-ground. These observations reinforce the concepts that the VHF pulses are produced by a breakdown process, while the optical pulses are the result of current flow. *INDEX TERMS*: 3304 Meteorology and Atmospheric Dynamics: Atmospheric electricity; 3324 Meteorology and Atmospheric Dynamics: Lightning; 3359 Meteorology and Atmospheric Dynamics: Radiative processes; 3360 Meteorology and Atmospheric Dynamics: Remote sensing; *KEYWORDS*: atmospheric electricity, lightning, remote sensing

Citation: Boeck, W. L., D. M. Suszcynsky, T. E. Light, A. R. Jacobson, H. J. Christian, S. J. Goodman, D. E. Buechler, and J. L. L. Guillen (2004), A demonstration of the capabilities of multisatellite observations of oceanic lightning, *J. Geophys. Res.*, 109, D17204, doi:10.1029/2003JD004491.

1. Introduction

[2] Over the last decade, the maturation of satellite-based observations of lightning has been marked by the successful operation of three major sensor packages: the Optical Transient Detector (OTD) sensor operated by the National Aeronautics and Space Administration (NASA) in the mid-1990s, the Lightning Imaging Sensor (LIS) and associated meteorological instrumentation currently operated by NASA aboard the Tropical Rainfall Measuring Mission (TRMM) spacecraft, and a suite of radio frequency (VHF) and optical instrumentation aboard the Fast On-Orbit Recording of Transient Events (FORTE) satellite currently operated by the National Nuclear Security Agency/Los Alamos National Laboratory/Sandia National

Laboratories (NNSA/LANL/SNL). Each of these programs has made fundamental advances in the science and engineering of space-based lightning detection [*Jacobson et al.*, 1999, 2000; *Boccippio et al.*, 2000a, 2000b, 2000c, 2002; *Buechler et al.*, 2000; *Suszcynsky et al.*, 2000, 2001; *Light et al.*, 2001a; *Light and Jacobson*, 2002; *Jacobson and Shao*, 2002; *Christian et al.*, 2003], and each has uniquely excelled in particular aspects of satellite-based lightning detection.

[3] The purpose of the current paper is to demonstrate that multiphenomenology, multisensor observations of lightning from space using the FORTE and TRMM spacecraft data sets together can provide a detailed picture of lightning phenomenology on both stroke (pulse) and flash timescales. Collectively, the sensors allow us to detect, locate, measure, analyze and classify lightning on a global basis. The results show that stroke level data can be examined in the context of a flash, which, in turn, can be physically located within a storm cloud providing some additional information on the cloud conditions.

2. Lightning Instrument Description

[4] The TRMM satellite was launched on 28 November 1997 to advance the state of the art in space-based lightning detection and contribute to NASA's Earth Observing System (EOS) program to study climate variability and change

¹Computer and Information Sciences Department, Niagara University, Lewiston, New York, USA.

²Space and Remote Sensing Sciences Group, Los Alamos National Laboratory, Los Alamos, New Mexico, USA.

³Global Hydrology and Climate Center, National Space Science Technology Center, Huntsville, Alabama, USA.

⁴Earth System Science Center, University of Alabama, Huntsville, Alabama, USA.

⁵Sensors and Electronics Department, Sandia National Laboratories, Albuquerque, New Mexico, USA.

Table 1. Summary of FORTE/TRMM Coincident Storms^a

Storm	Flash Content	Date	UT	Coordinates	Location
A	1 IC	16 July 1998	1205	−5.6N, 161.8E	Pacific Ocean
B	2 negative CG, 4 IC	5 April 2001	2117	−13.2N, 48.1E	near Madagascar
C	1 CG	12 July 2001	0758	−37.5N, 127.8E	South of Australia
D	1 positive CG	22 May 2001	1037	−32.9N, −107.6E	off west coast South America
E	5-cell MCS; 4 negative CG, 17 IC	20 September 2001	0622	26N, −92E	Gulf of Mexico

^aFORTE, Fast On-Orbit Recording of Transient Events; TRMM, Tropical Rainfall Measuring Mission; IC, intracloud discharge; CG, cloud-to-ground discharge; and MCS, mesoscale convective system.

[see e.g., *Christian et al.*, 1992]. The satellite's instrument complement includes the TRMM Microwave Imager (TMI), the Visible and Infra-Red Scanner (VIRS), and the first space-borne Precipitation Radar (PR), as well as the LIS. The LIS sensor, like its predecessor the OTD, is a charged coupled device (CCD) imager. The particularly low orbit of LIS (350 km) has resulted in the highest spatial resolution (4 km), geolocation accuracy (4 km), and detection efficiency of any space-based optical imager. LIS operates continuously with a 2 ms pixel integration time observing a large region (600 × 600 km) of the Earth's surface. All pixel data that exceed a threshold level is relayed to Earth for filtering and analysis. Further information on the TRMM instruments and results is given by *Kummerow et al.* [1998, 2000].

[5] The FORTE satellite is a joint LANL/SNL experiment that was launched into a nearly circular 825 km orbit on 29 August 1997. Unlike LIS, because the payload is operated in an experimental fashion, FORTE is routinely reconfigured for various data collection campaigns. FORTE carries a two-sensor Optical Lightning System (OLS) and broadband VHF receiver. The spacecraft systems are described by *Roussel-Dupre et al.* [2001].

[6] The FORTE optical system (OLS) is composed of a triggered broadband silicon photodiode detector (PDD) that collects high time resolution (15 μs) waveforms of lightning activity [*Kirkland et al.*, 2001], and a CCD imager, derived from the LIS design, called the LLS, that provides geolocation of events to within a pixel size of 10 km × 10 km [*Suszcynsky et al.*, 2001]. The PDD optical waveforms can be correlated with both the LLS and VHF records [*Suszcynsky et al.*, 2000; *Light et al.*, 2001a]. The FORTE VHF receivers can be configured to collect broadband VHF waveforms over various frequency bands within the 20 to 300 MHz frequency range. The FORTE Data Acquisition System contains enough memory for up to 0.8 s (cumulative) of 12-bit data. The VHF waveforms have proven to be effective tools for identifying certain lightning flash features (e.g., return strokes, leader activity, in-cloud activity) based solely on the frequency-time spectrograms (or power versus time profiles) [*Suszcynsky et al.*, 2000].

[7] In general, the TRMM instruments are designed for high spatial resolution continuous coverage on millisecond timescales. The FORTE instruments are routinely reconfigured to sample selected area targets with individual instruments independently triggering on microsecond timescales. The method for finding possibly coincident data begins with a monthly list of time intervals when the platforms are within 2200 km of each other. This set of times is used to search for FORTE VHF events recorded when there is a possible spatial coincidence. The times of the VHF events are then used to search the LIS orbit files for temporally

coincident data within a few millisecond window. The location data for the few resulting cases remaining are examined in detail to eliminate accidental coincidences. Using this procedure, we have identified examples of lightning from five oceanic thunderstorms jointly observed by FORTE and TRMM from 1998 to 2001.

3. Results

[8] The available data include examples of lightning from five oceanic thunderstorms. These storms range in intensity from single cell storms with a flash rate of one flash per minute to a mesoscale convective system (MCS) with five active cells. A brief summary of each storm is given in Table 1. The examples in this paper are selected from the MCS (storm E) because additional ancillary data are available for this storm system.

3.1. Stroke Level Data

[9] Twenty-one flashes in storm E were observed while FORTE's VHF receiver was slaved to trigger upon a PDD trigger. Two flashes are selected with 21 VHF/PDD coincident waveforms. The plots in Figure 1 show a detailed timing comparison of eight of these 21 VHF/PDD pairs. Each plot indicates the flash number (identification numbers derived from LIS flash counts for the entire orbit) and the PDD event letter within the flash (allowing comparison with the full sets of data presented in Figures 2 and 3). These plots show 2 ms of broadband optical irradiance and 4 ms of VHF power (square of electric field, E^2), normalized in the vertical dimension for convenient overlay. The delay of the optical pulse with respect to the VHF pulse is composed of a physical delay as well as broadening due to multiple scattering of the light flash by snow and ice crystals in the upper part of the storm [see, e.g., *Thomason and Krider*, 1982; *Light et al.*, 2001b]. The delays can be calculated by the technique described by *Light et al.* [2001a] for distinct in-cloud events. The general characteristics of coincident imager/photodiode/VHF detection of lightning activity have been presented in detail [*Suszcynsky et al.*, 2001]. Examples 203 A and B are examples of National Lightning Detection Network (NLDN) negative return strokes. These examples show progressively increasing negative leader VHF power preceding a large VHF impulse at the time of the return stroke's attachment to ground, followed by a reduction in VHF noise. Each is followed by a single optical pulse. The NLDN determined the peak current of 203 A was −101.9 kA and −33.3 kA for 203 B. The VHF patterns for 203 D and 203 E are more complex, but 203 E would be classified as a negative return stroke under the criteria of *Light et al.* [2001a], and indeed, NLDN reported 203 E to be a −30.8 kA ground stroke.

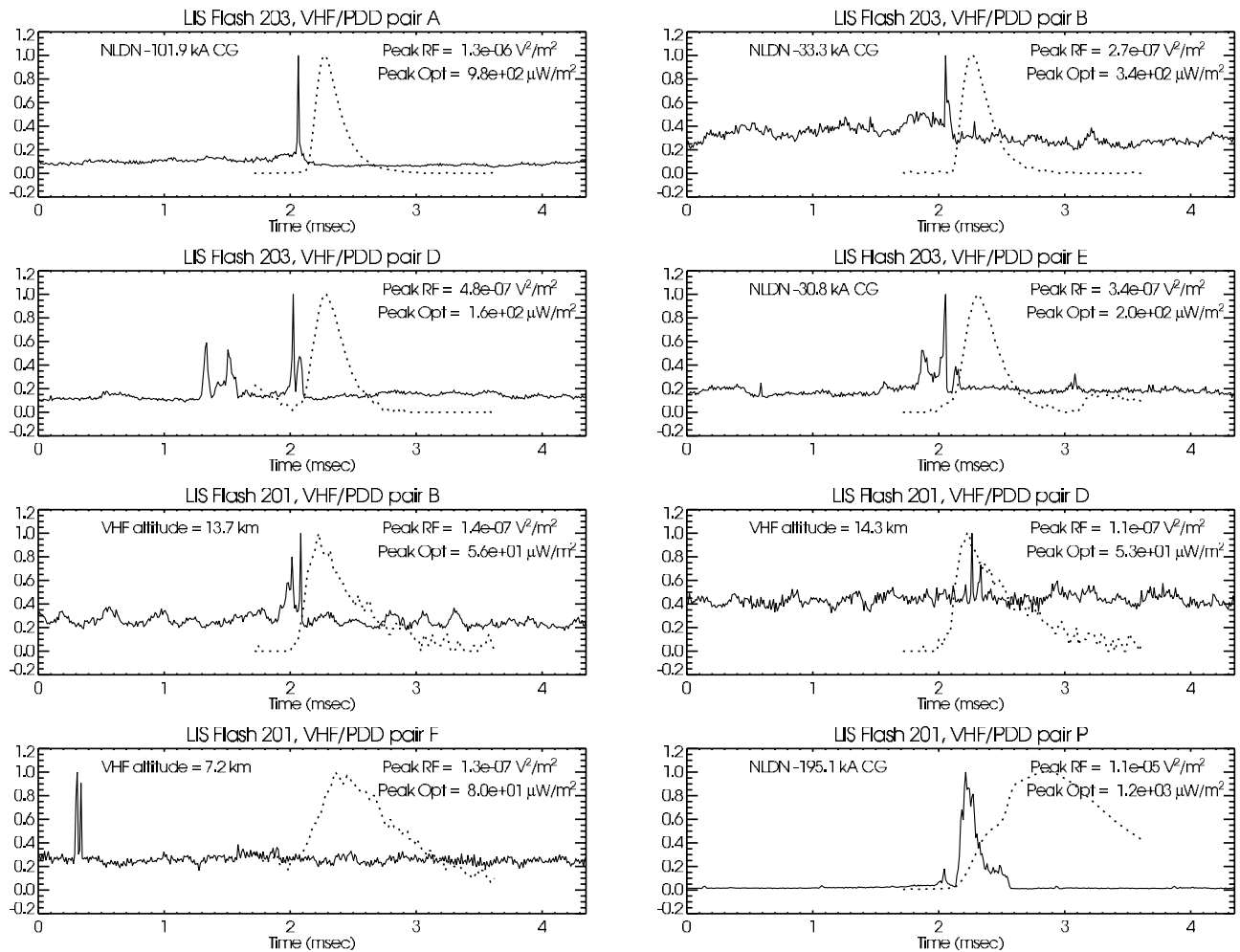


Figure 1. Plot of broadband optical pulse irradiance (dotted line) and VHF power (E^2 , solid line) for a selection of Fast On-Orbit Recording of Transient Events (FORTE)–observed events in Lightning Imaging Sensor (LIS) flashes 201 and 203 from storm E. The vertical axes have been individually normalized for convenient overlay, but the original scales can be reconstructed using the peak values labeling each plot. Each plot also indicates the LIS flash during which the event occurred and other information of interest regarding each event, namely, National Lightning Detection Network (NLDN) peak current estimate or VHF event altitude.

[10] In Figure 1, there are also VHF/PDD examples from flash 201. The FORTE satellite frequently observes impulsive pairs of VHF signals, like those seen in 201 B, 201 D, and 201 F, which have been called “Transionospheric Pulse Pairs” in previous studies [e.g., *Massey and Holden, 1995; Holden et al., 1995*]. The first pulse is interpreted as an in-cloud impulsive VHF emission that transits along a direct path to the satellite; the second pulse is the reflection of the source pulse from the Earth’s surface. The delay between the source pulse and its reflection is produced by the differing propagation path lengths. The source location, the satellite location, and the delay between the source and reflected pulses completely define the detection geometry and result in an absolute measurement of the height of the VHF source [*Jacobson et al., 1999*]. The VHF pulses in 201 B, 201 D, and 201 F originated at 13.7 km, 14.3 km, and 7.2 km above the water, respectively. Example 201 B shows an initial pulse superimposed on other VHF activity followed by a strong reflected pulse. Along with these

in-cloud VHF emissions, the PDD optical sensor observes continuing or overlapping optical pulses that may or may not have the same origin as the VHF activity. Examples 201 D and 201 F show cases where the timing does not imply a coincident VHF/PDD source location. Example 201F shows a pulse pair well in advance of the optical pulse, while 201D show an optical pulse that begins before the VHF pulses. Plot 201 P shows a ground stroke with complex VHF structure and a broad unresolved double optical pulse. NLDN reported 201 P to be a -195.1 kA ground stroke. All the data pairs for these storms were optically triggered and are therefore unlikely to include a particular class of very strong, impulsive in-cloud VHF events [*Light and Jacobson, 2002; Jacobson and Light, 2003*] that have been inferred to emit very little light. In 60 out of 73 4-ms VHF records from storm E, there is a credible VHF pulse immediately preceding the optical pulse. For these cases, which include CG strokes, we can suggest a cause and effect relationship. In 13 other cases,

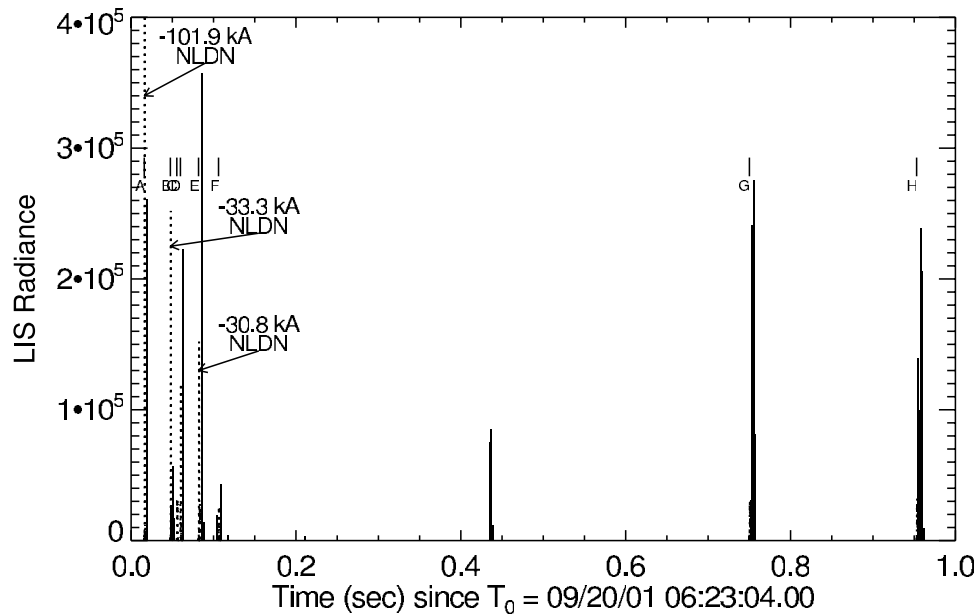


Figure 2. LIS and photodiode detector (PDD) amplitudes for pulses observed from LIS flash 203. LIS and PDD versus time in seconds after 0623:04 UTC are shown. LIS pulse amplitude is in red, and PDD waveforms (which appear compressed to instantaneous spikes on this timescale) are in black. The vertical scale of the PDD waveforms has been scaled for convenient overlay onto the LIS pulses. There were 24 LIS pulses and 8 PDD pulses observed from this flash. The time and estimated peak current of strokes recorded by the NLDN and spatially and temporally coincident with this flash are also indicated. This flash occurred at 25.29 north latitude, -91.48 east longitude and covered a footprint of 1250 km^2 on the ground. See color version of this figure at back of this issue.

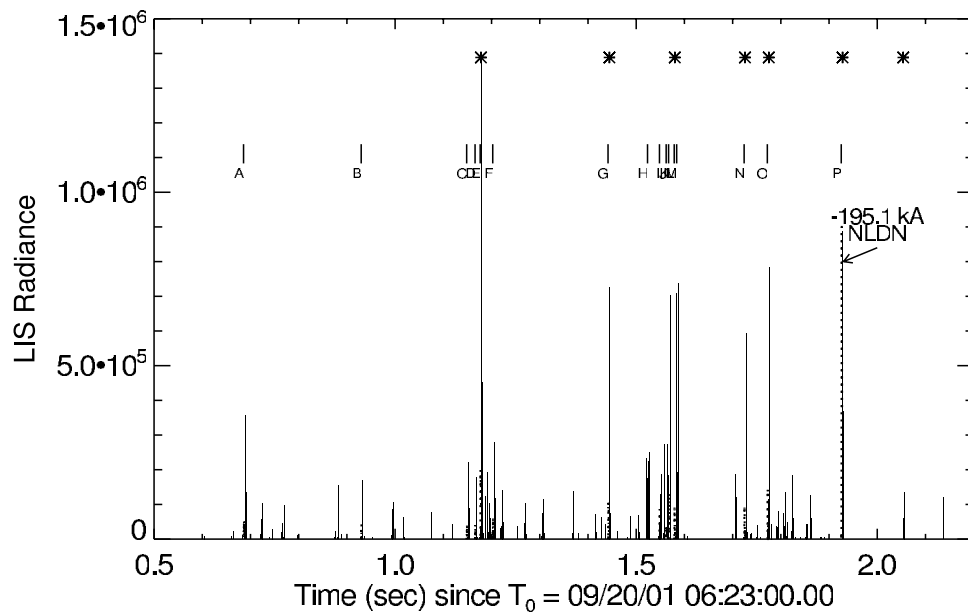


Figure 3. LIS and PDD amplitudes for pulses observed from LIS flash 201. LIS and PDD versus time in seconds after 0623:00 UTC are shown. LIS pulse amplitude is in red, and PDD waveforms (which appear compressed to instantaneous spikes on this timescale) are in black. The vertical scale of the PDD waveforms has been scaled for convenient overlay onto the LIS pulses. There were 150 LIS pulses, 16 PDD pulses, and 7 LLS pulses observed from this flash. The asterisks mark the times the LLS provided geolocation data coincident with LIS. The time and estimated peak current of a stroke recorded by the NLDN and spatially and temporally coincident with this flash are also indicated. This flash occurred at 26.06 north latitude, -91.79 east longitude and covered a footprint of 2810 km^2 on the ground. See color version of this figure at back of this issue.

the timing record does not imply causality. These observations reinforce the concepts that the VHF pulses are produced by a breakdown process while the optical pulses are the result of current flow.

3.2. Flash Level Data

[11] The data structure of a LIS orbit file organizes optical stroke level data into flashes on a storm-by-storm basis. The LIS flash product provides a flash level view of the two dimensional development of the optical pulses in a flash as a function of time. After accounting for time delays internal to the instruments and time of flight for each data stream, the FORTE PDD pulses can be plotted on the same continuous UTC timescale with the LIS data. The more sensitive threshold of LIS provides much more detail than PDD including the starting time and duration of the flash in the upper region of the thunderstorm.

[12] In Figures 2 and 3, temporal alignment between the LIS data stream and individual PDD records is shown on the timescale of extended flashes. The geolocation information from FORTE LLS is sufficient to confirm spatially coincident source locations and unambiguously assign PDD data to a specific LIS flash. For the seven joint LIS/LLS detections in flash 201, we find a mean distance offset of 13 km between geolocations from the two platforms. The spatial and temporal agreement of the LLS and LIS triggers in concert with the characteristic timing relationships between the LLS, PDD, and VHF waveforms verify that all four instruments recorded the same lightning flash.

[13] The LIS and PDD optical data for flash 203 and flash 201 are plotted using LIS amplitude units in Figures 2 and 3, respectively. LIS data are in red. UTC time is determined by adding the fractional second value from the horizontal axis to the UTC time printed below the chart. The 2-ms duration PDD waveforms from Figure 1 appear as black spikes on these flash duration timescales which can be over a second long. The asterisks mark the times that a FORTE LLS geolocation is available, and any NLDN ground strokes recorded from this flash have their time and peak amplitude indicated as well. The latitude and longitude values are the centroid of the optical footprint as recorded by LIS. The PDD and LIS units of measurement are not identical (broadband versus narrowband optical); consequently, the PDD data were scaled to a value convenient for display.

[14] Figure 2 presents the complete time series of data for LIS flash 203, in which the LIS recorded 24 optical pulses. During this flash, the PDD triggered 8 times at pulses labeled A–H. Four of the VHF/PDD data pairs shown in Figure 1 were selected from this flash. Note that the CG activity occurred early in the time history of this flash. The optical footprint of this flash covered 1250 km².

[15] Figure 3 shows time development of a complex flash (LIS 201) with duration of 1.53 sec. LIS recorded 150 optical pulses, 16 of which (labeled A–P) were captured by PDD. The animation of this flash shows the luminosity begins at one location and extends to cover a footprint of 2800 km² before connecting to ground at a location near the start. NLDN reported this as a –195.1 kA negative CG flash. As described in section 3.1, three sample VHF pulse pairs from flash 201 allow us to determine that

Table 2. PDD Detection Ratio Relative to LIS, as a Function of LIS-Detected Pulse Amplitude^a

LIS Amplitude	PDD Detected	LIS Detected	PDD/LIS, %
10 ⁶ –10 ⁷	4	4	100
10 ⁵ –10 ⁶	48	108	44
10 ⁴ –10 ⁵	40	435	9
10 ³ –10 ⁴	0	155	0

^aPDD, photodiode detector; LIS, Lightning Imaging Sensor.

VHF emissions within this flash occurred at 13.7, 14.3 and 7.2 km above the seawater.

[16] In all cases where the active cell was within the TRMM precipitation radar field of view, precipitation was found at the calculated altitudes. Several two dimensional time animations of LIS event locations were produced to study the development of individual flashes. Animations may be viewed at http://nis-www.lanl.gov/nis-projects/forte_science/html/co_rf.html.

[17] A summary of the comparative detection of nighttime optical pulses between the broadband FORTE photodiode (PDD) and the narrowband optical CCD on LIS is given in Table 2. Both instruments are detection limited by threshold settings which are minimized and constant during local night.

3.3. Storm Level Data

[18] When the two dimensional pixel data from LIS are examined in concert with the other TRMM instruments, each flash can be placed in its storm context. Most flashes begin and end at the location of a storm dynamic feature such as an updraft. These localized flashes produce an approximately circular optical footprint. For example, in cell 1, there are 10 VHF source height determinations from several flashes (9.8, 13.4, 13.1, 13.0, 12.5, 9.6, 8.3, 13.9, 14.5, 10.3 km) which are in good agreement with the height of precipitation measure by TRMM PR. Some flashes in other cells show extensive horizontal migration.

[19] The flashes chosen for this paper occurred in storm E (see Table 1), a cluster of thunderstorms located south of Louisiana. This cluster consisted of a number of thunderstorms, five of which were actively produced lightning as observed by LIS and FORTE. Examination of NLDN data showed that the cells within this cluster produced CG lightning for 7 hours. The cells moved toward the southwest over this time period. Nearby buoy data indicated that the storms were fueled by warm (temperature of 28.9°C), moist (25.6°C dew point) surface air.

[20] Additionally, there are data from both the TRMM/VIRS and TRMM/TMI for this storm. The VIRS measures radiance from the visible through infrared (0.63, 1.6, 3.75, 10.8, 12.2 μm) portion of the spectrum. The VIRS swath width is 720 km with a nadir resolution of 2.2 km. The TMI is a nine-channel passive microwave radiometer that measures the amount of radiation emitted from the Earth's surface and atmosphere at 10.7, 19.4, 21.3, 37.0, and 85.5 GHz, which is then converted to brightness temperatures via the Planck law. The TMI swath width is 785 km with footprints ranging from ~35 km² (at 85.5 GHz) to ~2330 km² (at 10.7 GHz) [Kummerow *et al.*, 1998]. Low polarization-corrected temperatures (PCT) at 37 GHz and 85.5 GHz in a cloud are indicative of precipitation-sized ice particles such as found in deep convection [Wu and

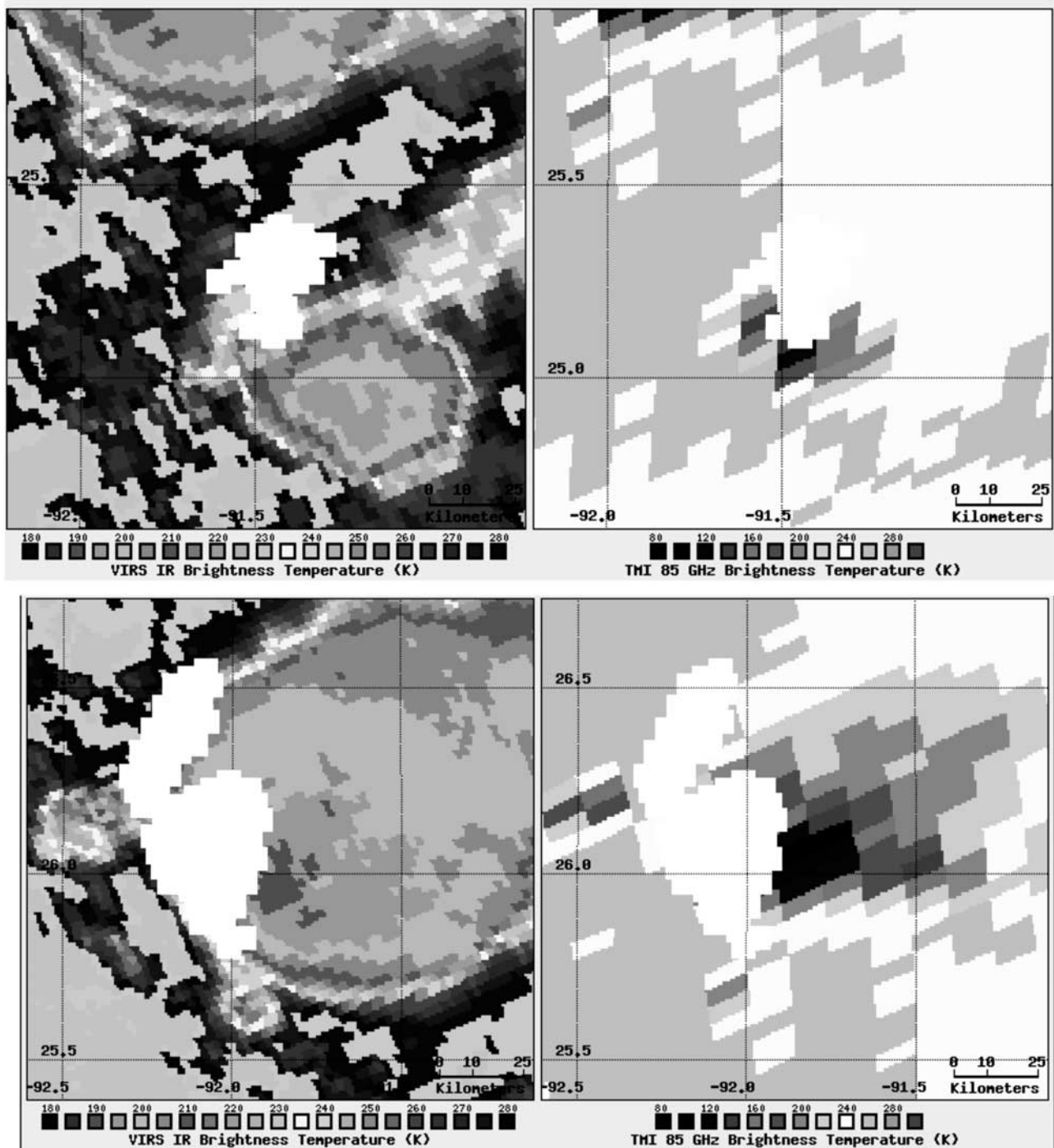


Figure 4. (top) TRMM Visible and Infra-Red Scanner (VIRS) IR channel (left), TRMM Microwave Imager (TMI) 85 GHz channel (right) and the LIS optical footprint (white areas in both the VIRS and TMI plots) for flash 203 at the time of the first return stroke. (bottom) Same observations for flash 201. See color version of this figure at back of this issue.

Weinman, 1984]. The PCT at 85 GHz is not a true temperature measurement, but it is a consistent marker of the location of the precipitation core at about 10 km altitude under the thunderstorm anvil. Results from TOGA CORE [Petersen *et al.*, 1996] show that very little lightning is expected in an oceanic environment. An analysis of LIS data [Toracinta *et al.*, 2002] shows that the frequency of lightning observable by LIS ranges from less than 10% for

microwave PCT temperatures near 200 K to nearly 100% for microwave temperatures less than 160K.

[21] The LIS optical footprint of flash 203 at the time of the first return stroke is shown superimposed on the 10.8 μm IR and 85 GHz images in Figure 4 top plots (white area). The left plots are the 10.8 μm IR view of the cloud top temperatures from VIRS. The right plots are the TMI 85 GHz scan for cells 4 and 2. The apparently cold areas

Table 3. Flashing Duty Cycle for Locations in MCS Storm E

Location	Cell History	Flashing Duty Cycle, %
Cell 1	recent developed cell upstream of the main cell	8.41
Cell 2	main cell, with large cold core	22.77
Cell 3	most recent developing cell upstream of cell 1	1.47
Location 4	between main cell and older cell 4 to south	0.99
Location 5	in anvil of main cell	0.68

are produced by the characteristic scattering of upwelling microwave radiation due to ice crystals. This flash occurred in a location near but not in the cold core of this cell.

[22] Similarly, Figure 4 bottom plots show the storm environment of the largest precipitation core of the MCS (cell 2), as detected by VIRS and TMI, with flash 201 at its edge. This core was the source of active lightning from 0200 to 0900 UTC. Flash 201 is a complex flash lasting nearly 1.5 s. LIS recorded 148 out of 150 optical pulses near the cold core before the ground stroke. Although the footprint was 2800 km², the ground stroke was in the vicinity of the starting position of the flash and illuminated an area in the anvil away from the cold core and previous activity.

3.4. Storm Charging Rate

[23] Simple flash counts ignore the duration of discharge processes and may not be a sufficient measure of discharging rate. The LIS algorithm assumes the dark times between the pulses detected by LIS are due to activities deep in the cloud that are undetected by LIS. If one assumes that a mature cell can not store additional electrical energy, then the discharge rate will track the charging rate. As a rough measure of the relative storm cell charging rate, we will therefore examine the flashing duty cycle (FDC) for all the cells and locations of interest in the MCS of storm E. The FDC is defined as a dimensionless ratio of the total of duration of all LIS flashes at a location, divided by the LIS observation time of the area, as shown in Table 3. The FDC could be used to estimate a charging rate by multiplying the FDC ratio by the estimated discharging current. The order of magnitude difference in FDC between the active cells and the cloud anvil is consistent with current understanding of storm electrification processes.

4. Conclusion

[24] We have identified examples of lightning in five nighttime, oceanic thunderstorms which were jointly observed by TRMM and FORTE. The multiplicity of instruments on board these satellites presents a multiphenomenological snapshot view of oceanic nighttime convection. Some of the storms show PCT temperatures below 180K, which are characteristic signatures of a frozen convective cloud core.

[25] Two independent optical imagers establish the flash locations for lightning that is detected by the two satellites. The spatial-temporal agreement of the FORTE/LLS and TRMM/LIS triggers is excellent. The PDD data also show the broadening and delay of the optical pulses due to scattering by several kilometers of cloud along the ray path. The relative fraction of LIS-detected optical pulses that

were also observed by the FORTE/PDD scales proportionally with the optical pulse amplitude.

[26] The FORTE/VHF data sometimes allow estimation of the VHF source emissions heights and identification of individual discharge processes as positive or negative, in-cloud or cloud-to-ground. The TRMM TMI, VIRS, and PR provide storm contexts for the lightning observations. In cases where FORTE/VHF data provide VHF emission heights and TRMM/PR data are also available, precipitation is found at the calculated altitudes. In the cases where TRMM provides meteorological context for the lightning, it appears that the lightning originates near, but not in, the cold storm cores.

[27] In summary, multiphenomenology, multisensor observations of lightning from space using the FORTE and TRMM spacecraft provide a detailed picture of lightning phenomenology on both stroke (pulse) and flash timescales. Collectively, the sensors allow us to detect, locate, measure, analyze and classify lightning on a global basis and provide good argument for outfitting future satellite-based global lightning monitors with optical imaging and VHF sensors.

[28] **Acknowledgments.** The authors would like to thank Diane Roussel-Dupre of Los Alamos National Laboratory, Dennis Boccippio of NASA/MSFC, Doug Mach of UAH, Jeff Green and Bill Myre of Sandia National Laboratories, and the rest of the FORTE and LIS Science and Operations Teams for essential discussions, comments, and technical support. We thank the reviewers for their insightful comments. NLDN data were provided by the NASA Lightning Imaging Sensor (LIS) instrument team and the LIS data center via the Global Hydrology Resource Center (GHRC) located at the Global Hydrology and Climate Center (GHCC), Huntsville, Alabama, through a license agreement with Vaisala-Global Atmospheric, Inc. The data available from the GHRC are restricted to LIS science team collaborators and to NASA EOS and TRMM investigators.

References

- Boccippio, D. J., K. L. Cummins, H. J. Christian, and S. J. Goodman (2000a), Combined satellite- and surface-based estimation of the intracloud-cloud-to-ground lightning ratio over the continental United States, *Mon. Weather Rev.*, *129*, 108–122.
- Boccippio, D. J., S. J. Goodman, and S. Heckman (2000b), Regional differences in tropical lightning distributions, *J. Appl. Meteorol.*, *39*, 2231–2248.
- Boccippio, D. J., K. Driscoll, W. Koshak, R. Blakeslee, W. Boeck, D. Buechler, H. Christian, and S. Goodman (2000c), The Optical Transient Detector (OTD): Instrument characteristics and cross-sensor validation, *J. Atmos. Oceanic Technol.*, *17*, 441–458.
- Boccippio, D. J., W. J. Koshak, and R. J. Blakeslee (2002), Performance assessment of the Optical Transient Detector and Lightning Imaging Sensor. Part I: Predicted diurnal variability, *J. Atmos. Oceanic Technol.*, *19*, 1318–1332.
- Buechler, D. E., K. Driscoll, S. J. Goodman, and H. J. Christian (2000), Lightning activity within a tornadic thunderstorm observed by the Optical Transient Detector (OTD), *Geophys. Res. Lett.*, *27*, 2253–2256.
- Christian, H. J., S. J. Goodman, and R. J. Blakeslee (1992), Lightning Imaging Sensor (LIS) for the Earth Observing System, *NASA Tech.*, *4350*.

- Christian, H. J., et al. (2003), Global frequency and distribution of lightning as observed from space by the Optical Transient Detector, *J. Geophys. Res.*, *108*, 4005, doi:10.1029/2002JD002347.
- Holden, D. N., C. P. Munson, and J. C. Devenport (1995), Satellite observations of transionospheric pulse pairs, *Geophys. Res. Lett.*, *22*, 889–892.
- Jacobson, A. R., and T. E. Light (2003), Bimodal radio frequency pulse distribution of intracloud lightning signals recorded by the FORTE satellite, *J. Geophys. Res.*, *108*, 4266, doi:10.1029/2002JD002613.
- Jacobson, A. R., and X. M. Shao (2002), FORTE satellite observations of very narrow radiofrequency pulses associated with the initiation of negative cloud-to-ground lightning strokes, *J. Geophys. Res.*, *107*(D22), 4661, doi:10.1029/2001JD001542.
- Jacobson, A. R., S. O. Knox, R. Franz, and D. C. Enemark (1999), FORTE Observations of lightning radio-frequency signatures: Capabilities and basic results, *Radio Sci.*, *34*, 337–354.
- Jacobson, A. R., K. L. Cummins, M. Carter, P. Klingner, D. Roussel-Dupre, and S. O. Knox (2000), FORTE radio-frequency observations of lightning strokes detected by the National Lightning Detection Network, *J. Geophys. Res.*, *105*, 15,653–15,658.
- Kirkland, M. W., D. M. Suszcynsky, R. Franz, J. L. L. Guillen, and J. L. Green (2001), Optical observations of terrestrial lightning by the FORTE satellite photodiode detector, *J. Geophys. Res.*, *106*, 3499–3510.
- Kummerow, C., W. Barnes, T. Kozu, J. Shiue, and J. Simpson (1998), The Tropical Rainfall Measuring Mission (TRMM) sensor package, *J. Atmos. Oceanic Technol.*, *15*, 809–817.
- Kummerow, C., et al. (2000), The status of the Tropical Rainfall Measuring Mission (TRMM) after two years in orbit, *J. Appl. Meteorol.*, *39*, 1965–1982.
- Light, T. E., and A. R. Jacobson (2002), Characteristics of impulsive VHF lightning signals observed by the FORTE satellite, *J. Geophys. Res.*, *107*(D24), 4756, doi:10.1029/2001JD001585.
- Light, T. E., D. M. Suszcynsky, and A. R. Jacobson (2001a), Coincident radio frequency and optical emissions from lightning observed with the FORTE satellite, *J. Geophys. Res.*, *106*, 28,223–28,231.
- Light, T. E., D. M. Suszcynsky, M. W. Kirkland, and A. R. Jacobson (2001b), Simulations of lightning optical waveforms as seen through clouds by satellites, *J. Geophys. Res.*, *106*, 17,103–17,114.
- Massey, R. S., and D. N. Holden (1995), Phenomenology of transionospheric pulse pairs, *Radio Sci.*, *30*, 1645–1659.
- Petersen, W. A., S. A. Rutledge, and R. E. Orville (1996), Cloud-to-ground lightning observations from TOGA CORE: Selected results and lightning location algorithms, *Mon. Weather Rev.*, *124*, 602–620.
- Roussel-Dupre, D., P. Klingner, L. Carlson, R. Dingler, and D. Esch-Mosher (2001), Four years of operations and results with FORTE, paper presented at AIAA Space 2001 Conference, Am. Inst. of Aeronaut. and Astronaut., Albuquerque, N. M., 28–30 Aug.
- Suszcynsky, D. M., M. W. Kirkland, A. Jacobson, R. Franz, S. Knox, J. L. Guillen, and J. Green (2000), FORTE observations of simultaneous RF and optical emissions from lightning: Basic phenomenology, *J. Geophys. Res.*, *105*, 2191–2201.
- Suszcynsky, D. M., T. E. Light, S. Davis, J. L. Green, J. L. L. Guillen, and W. Myre (2001), Coordinated observations of optical lightning from space using the FORTE photodiode detector and CCD imager, *J. Geophys. Res.*, *106*, 17,897–17,906.
- Thomason, L. W., and E. P. Krider (1982), The effects of clouds on the light produced by lightning, *J. Atmos. Sci.*, *39*, 2051–2065.
- Toracinta, E. R., D. J. Cecil, E. J. Zipser, and S. W. Nesbitt (2002), Radar, passive microwave, and lightning characteristics of precipitating systems in the tropics, *Mon. Weather Rev.*, *130*, 802–824.
- Wu, R., and J. A. Weinman (1984), Microwave radiances from precipitating clouds containing aspherical ice, combined phase, and liquid hydrometeors, *J. Geophys. Res.*, *89*, 7170–7178.

W. L. Boeck, Computer and Information Sciences Department, Niagara University, Niagara, NY 14109, USA. (boeck@niagara.edu)

D. E. Buechler, Earth System Science Center, University of Alabama in Huntsville, Huntsville, AL 35816, USA.

H. J. Christian and S. J. Goodman, Global Hydrology and Climate Center, National Space Science Technology Center, Huntsville, AL 35816, USA.

J. L. L. Guillen, Sensors and Electronics Department, Sandia National Laboratories, MS 0972, Albuquerque, NM 87185, USA.

A. R. Jacobson, T. E. Light, and D. M. Suszcynsky, Space and Remote Sensing Sciences Group (ISR-2), Los Alamos National Laboratory, MS D436, Los Alamos, NM 87545, USA.

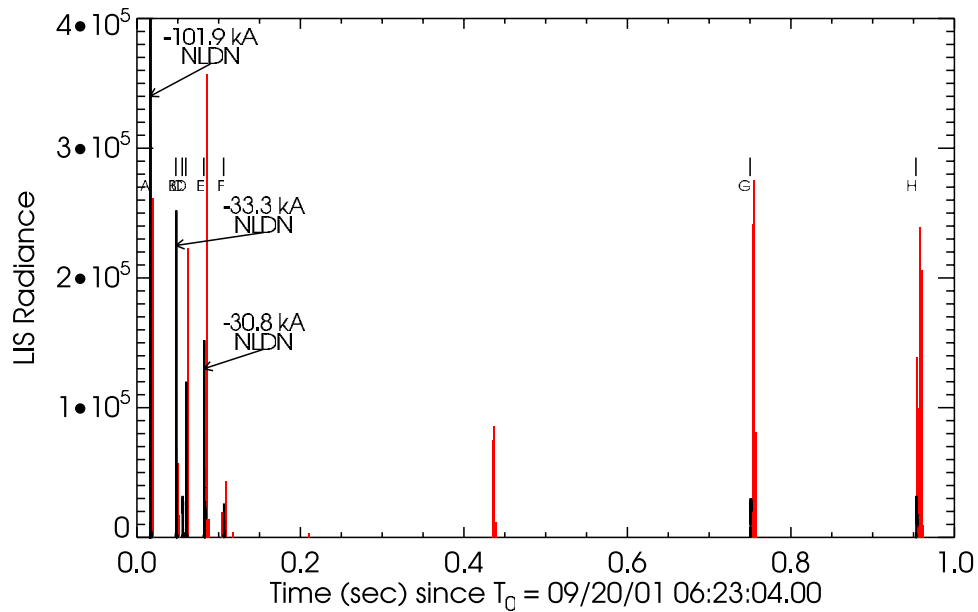


Figure 2. LIS and photodiode detector (PDD) amplitudes for pulses observed from LIS flash 203. LIS and PDD versus time in seconds after 0623:04 UTC are shown. LIS pulse amplitude is in red, and PDD waveforms (which appear compressed to instantaneous spikes on this timescale) are in black. The vertical scale of the PDD waveforms has been scaled for convenient overlay onto the LIS pulses. There were 24 LIS pulses and 8 PDD pulses observed from this flash. The time and estimated peak current of strokes recorded by the NLDN and spatially and temporally coincident with this flash are also indicated. This flash occurred at 25.29 north latitude, -91.48 east longitude and covered a footprint of 1250 km^2 on the ground.

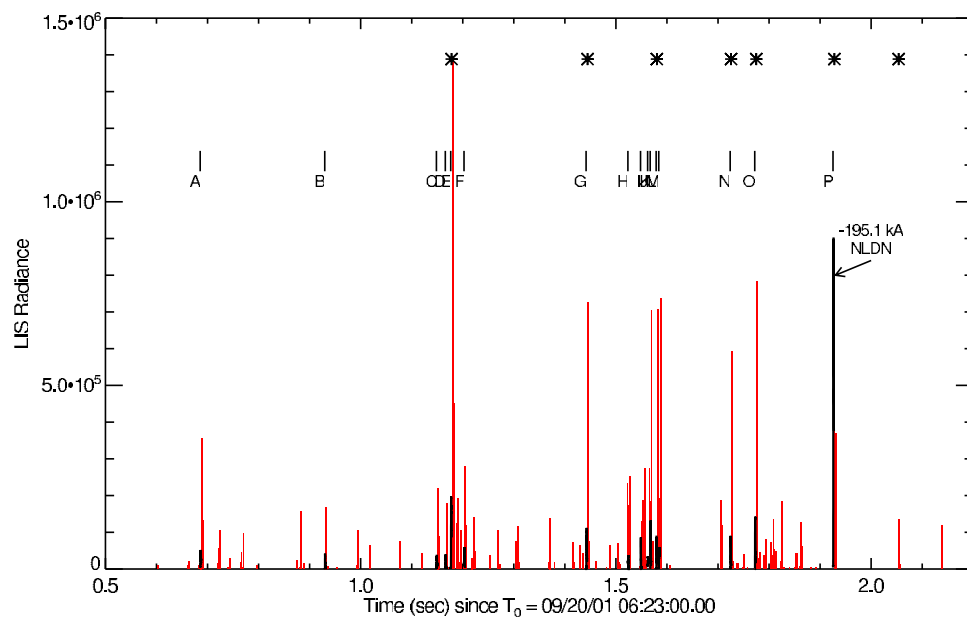


Figure 3. LIS and PDD amplitudes for pulses observed from LIS flash 201. LIS and PDD versus time in seconds after 0623:00 UTC are shown. LIS pulse amplitude is in red, and PDD waveforms (which appear compressed to instantaneous spikes on this timescale) are in black. The vertical scale of the PDD waveforms has been scaled for convenient overlay onto the LIS pulses. There were 150 LIS pulses, 16 PDD pulses, and 7 LLS pulses observed from this flash. The asterisks mark the times the LLS provided geolocation data coincident with LIS. The time and estimated peak current of a stroke recorded by the NLDN and spatially and temporally coincident with this flash are also indicated. This flash occurred at 26.06 north latitude, -91.79 east longitude and covered a footprint of 2810 km^2 on the ground.

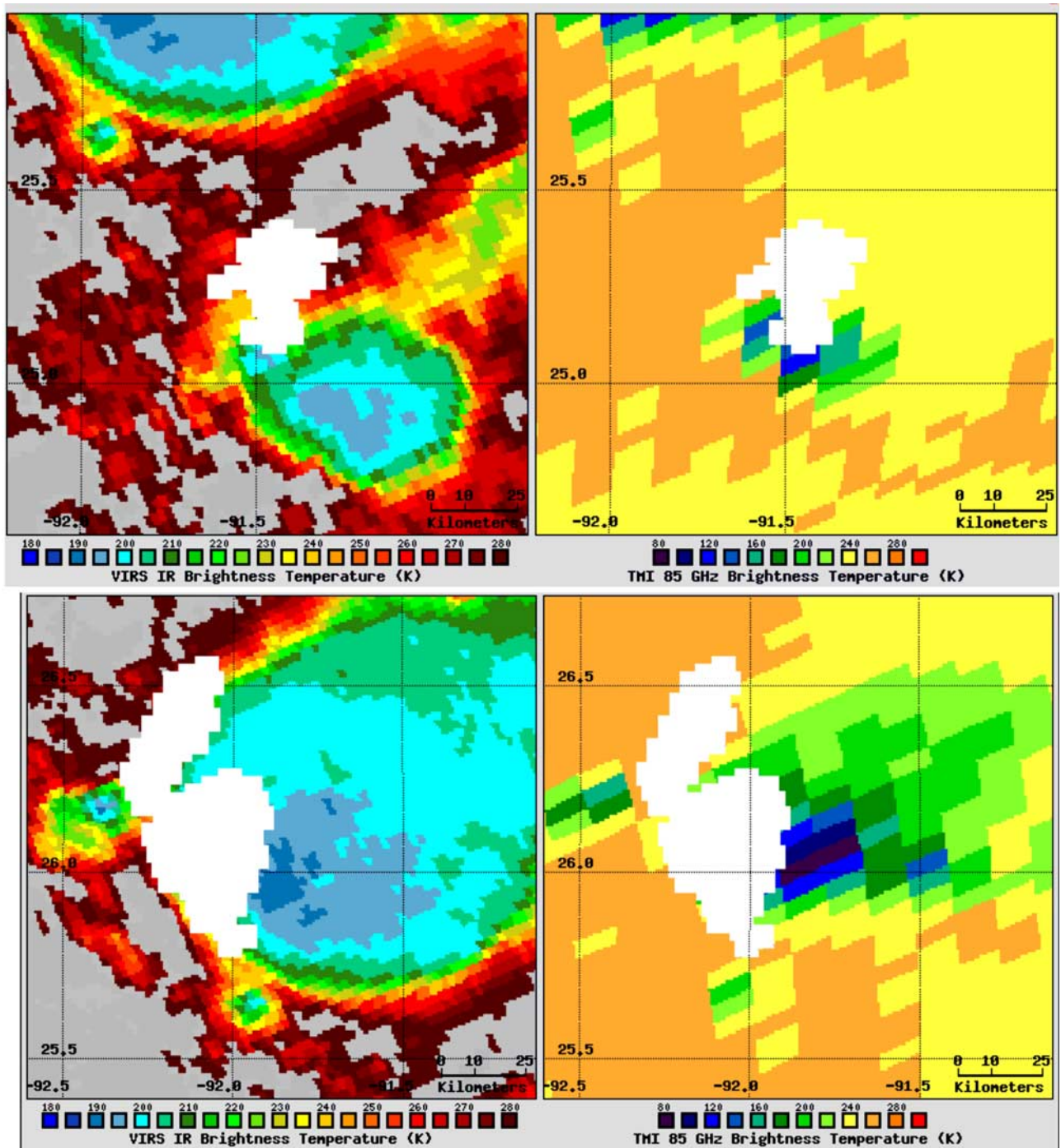


Figure 4. (top) TRMM Visible and Infra-Red Scanner (VIRS) IR channel (left), TRMM Microwave Imager (TMI) 85 GHz channel (right) and the LIS optical footprint (white areas in both the VIRS and TMI plots) for flash 203 at the time of the first return stroke. (bottom) Same observations for flash 201.